

Characterizing Exoplanets for Habitability

Tyler D. Robinson

Abstract A habitable exoplanet is a world that can maintain stable liquid water on its surface. Techniques and approaches to characterizing such worlds are essential, as performing a census of Earth-like planets that may or may not have life will inform our understanding of how frequently life originates and is sustained on worlds other than our own. Observational techniques like high contrast imaging and transit spectroscopy can reveal key indicators of habitability for exoplanets. Both polarization measurements and specular reflectance from oceans (also known as “glint”) can provide direct evidence for surface liquid water, while constraining surface pressure and temperature (from moderate resolution spectra) can indicate liquid water stability. Observations of variability (that indicates weather) from, as well as mapping of, exoplanets can provide indirect evidence of habitability, and measurements of water vapor or cloud profiles that indicate condensation near a surface could also provide evidence for habitability. Approaches to making the types of measurements that indicate habitability are diverse, and have different considerations for the required wavelength range, spectral resolution, maximum noise levels, stellar host temperature, and observing geometry.

Introduction

The emphasis on which planetary surface properties are key to determining habitability has, like many ideas in exoplanetary science, changed in time. Early work, even before the first detections of worlds around other stars, highlighted the importance of clement conditions at the planetary surface—Huang (1959) discussed the need for enough “heat” for organisms to survive, while Dole (1964) focused on a temperature range that would be suitable for humans. However, it has become

Tyler D. Robinson
Lunar and Planetary Laboratory, University of Arizona, Tucson, AZ 85721, USA, e-mail:
tdrobin@arizona.edu

widely accepted that liquid water played an essential role in the origin, development, and maintenance of life on Earth (e.g., Brack 1993), and, as a result, most studies of habitability have since focused on stable surface liquid water. Rasool and de Bergh (1970), in their early description of the runaway greenhouse and the evolution of climate on the terrestrial planets of the Solar System, were amongst the first to place a strong emphasis on stable surface liquid water. Similarly, in their study of the co-evolution of Earth and life, Hart (1978) required liquid water (as well as certain atmospheric composition constraints) for life to originate.

Foundational work on habitable zones around other stars (Hart 1979; Whitmire et al 1991; Kasting et al 1993) and on the emergence of habitable worlds (Matsui and Abe 1986; Abe and Matsui 1988) strongly emphasize that habitable planets are the subset of terrestrial worlds that can have stable surface liquid water. Of course, this does not rule out the potential for sub-surface habitable environments, such as the ocean beneath Europa's icy crust (Pappalardo et al 1999; Chyba and Phillips 2001)—the emphasis on *surface* habitability is based in pragmatism, as discovering and characterizing any sub-surface habitable environments on exoplanets (or exomoons) will likely remain unfeasible even into the distant future.

Motivated in large part by the success of NASA's *Kepler* mission (Borucki et al 2010) and the ever-growing number of known potentially-habitable exoplanets, many authors and groups have sought to refine our understanding of the myriad ways a planet can (or cannot) maintain habitability (Forget and Pierrehumbert 1997; Joshi et al 1997; Stevenson 1999; Selsis et al 2007; Haqq-Misra et al 2008; von Paris et al 2010; Abe et al 2011; Pierrehumbert and Gaidos 2011; Goldblatt et al 2013; Kopparapu et al 2013; Rugheimer et al 2013; Wordsworth and Pierrehumbert 2013; Wolf and Toon 2013; Leconte et al 2013; Yang et al 2013; Shields et al 2013; Zsom et al 2013; Ramirez and Kaltenegger 2014; Luger and Barnes 2015; Way et al 2016). These studies demonstrate a relatively well-developed understanding of *how* a world can be habitable. The next critical step towards undertaking a census of Earth-like planets around our nearest stellar neighbors is, then, developing techniques for remotely assessing the likelihood that an exoplanet could have stable surface liquid water or, in other words, the remote characterization of habitability.

Interestingly, Galileo was likely the first to consider the remote detection of surface liquid water when, in his *Dialogue Concerning the Two Chief World Systems*, he used the brightness of the dark portion of the lunar disk (which is illuminated by reflected light from Earth) to deduce that “seas would appear darker, and [...] land brighter” when observed from a distance (Galilei 1632). Modern discussions of techniques for the remote characterization of exoplanet habitability, which are the focus of this chapter, generally fall into three categories. First, surface liquid water could be directly detected using reflection and/or polarization measurements. Second, the surface pressure and temperature of an exoplanet could be inferred from spectroscopic observations, which then determines the stability of liquid water from its phase diagram. Finally, in the absence of such direct evidence for surface liquid water (or its stability), habitability would need to be constrained using some combination of photometric and spectroscopic observations and modeling to try to best understand the planetary surface environment.

The direct detection of surface liquid water and the inference of surface pressure and temperature were demonstrated for Earth by Sagan et al (1993) using observations from a pair of flybys performed by the *Galileo* spacecraft. Specular reflection, which is indicative of liquids, was detected with *Galileo* imaging, and solid phase water absorption was identified in observations of the polar caps, thereby providing strong evidence that the surface liquid is water. Near-infrared spectral observations of thermal emission from cloud-free regions of the planet revealed surface temperatures in the range 240–290 K, and a crude spectral retrieval analysis (Drossart et al 1993) indicated an integrated atmospheric column mass $>200 \text{ g cm}^{-2}$. For an Earth-like gravitational acceleration, this column mass corresponds to a surface pressure $>0.2 \text{ bar}$. Given the aforementioned range of surface temperatures, the surface (even for pressures much larger than the lower limit quoted here) spans the solid-to-liquid transition regime for water, and is, thus, habitable.

Sagan et al (1993) also present multiple strong lines of evidence for Earth being inhabited. This indicates that, for some worlds, it may prove easier to detect life than to detect habitability. It is, however, critical that approaches be developed which can be used to independently recognize both habitable as well as life-bearing planets. Employing these independent approaches, as part of a larger census of exoplanetary surface and atmospheric environments, will tell us if originating and sustaining life is common (where nearly all potentially habitable worlds are inhabited) or rare (where nearly all planets that show signs of habitability do not show signs of life). Either of these findings would tell us something profound about our place in the Universe.

From the perspective of exoplanet science, the Sagan et al (1993) *Galileo* results are missing a key complication—the habitability analyses all rely on spatially resolved observations. Generally, observations of exoplanets are spatially unresolved. Thus, for a true Pale Blue Dot, cloudy and clearsky, ocean and land, and warm and cold scenes would all be blended together, which significantly complicates our ability to characterize the surface environment for signs of habitability. Here, it must be emphasized that habitability is a *surface* phenomenon and can only be constrained if a remote observation has sensitivity to the surface (i.e., that some light at certain wavelengths in the observed spectral range comes from at/near the surface). In other words, we would have little hope of studying the surface environment of a terrestrial exoplanet that is enshrouded with completely opaque clouds.

The following sections present and synthesize studies related to the characterization of exoplanet habitability. For earlier reviews on characterizing terrestrial exoplanets which include some details on habitability, see Meadows (2010) Kaltenegger et al (2010). A complementary review of processes related to planetary habitability and its remote characterization can be found in Kopparapu et al (2020). In our review, we begin with an overview of the key observational techniques that can be used to remotely characterize exoplanets, and highlight the sizes of signatures relevant to studying Pale Blue Dots. Following this overview, we discuss how the different observational techniques can be used to directly detect surface liquid water, to measure surface pressure and temperature, and/or to place other key constraints on the planetary environment. Whenever possible, the feasibility of detecting habit-

ability indicators is discussed. We conclude by outlining several important questions that remain unaddressed on the topic of characterizing for habitability.

Observational Techniques

Several observational techniques are relevant to the characterization of the atmospheres and surface environments of potentially habitable exoplanets: transit spectroscopy, high contrast imaging, and secondary eclipse spectroscopy. We briefly review these here and demonstrate the relevant signal sizes. For an overview of techniques and signature sizes for a diversity of planet types, see Cowan et al (2015).

Transit Spectroscopy: In transit spectroscopy (Seager and Sasselov 2000; Brown 2001; Hubbard et al 2001), the small fractional dimming of an unresolved exoplanet host star is measured as the planet transits the stellar disk. This quantity—the transit depth—is usually interpreted as the square of the ratio of a characteristic planetary radius (R_p) to the stellar radius (R_s), and, when measured at different wavelengths, the transit depth indicates the planetary atmospheric opacity as the world will appear larger on the stellar disk at wavelengths that correspond to larger extinction. While the overall scale of the transit depth is given by $(R_p/R_s)^2$, the contrast of spectral features will depend on the altitude difference probed within versus outside a molecular band (Δz), and is approximately,

$$\frac{2\Delta z R_p}{R_s^2} \approx 0.6 \text{ ppm} \left(\frac{T}{250 \text{ K}} \right) \left(\frac{29 \text{ g mol}^{-1}}{\mu} \right) \left(\frac{5.5 \text{ g cm}^{-3}}{\rho_p} \right) \left(\frac{R_\odot}{R_s} \right)^2, \quad (1)$$

where T is a characteristic atmospheric temperature, μ is the atmospheric mean molar weight, and ρ_p is the planetary bulk density. We have assumed the altitude range probed is a few pressure scale heights, and we have adopted Earth-like values for all parameters. For early, mid, and late M dwarfs, the scale of features increases to 2, 10, and 60 ppm, respectively.

High Contrast Imaging: In high contrast (or “direct”) imaging (Traub and Oppenheimer 2010), optical techniques are used to resolve the faint point spread function of a planetary companion from that of its bright host. Typical approaches include coronagraphy (Guyon et al 2006; Mawet et al 2012), external occulters or “starshades” (Cash et al 2007; Shaklan et al 2010), and interferometry (Beichman et al 1999). The relevant measure is the planet-to-star flux ratio (F_p/F_s), which (roughly) sets the contrast that must be achieved to accomplish imaging (although planet-star angular separation, host star apparent magnitude, exozodiacal dust brightness, and other quantities also impact the feasibility of observation). For reflected light, which would be the focus of any near- or far-future direct imaging efforts, the flux ratio is given by $A_g \Phi(\alpha) (R_p/a)^2$, where A_g is the geometric albedo, Φ is the phase function (which depends on the phase angle, α), and a is the orbital distance. Assuming that the insolation on potentially habitable exoplanets is roughly that of what Earth

receives ($S_{\oplus} = 1360 \text{ W m}^{-2}$), we have,

$$\frac{F_p}{F_s} \approx 1 \times 10^{-10} \left(\frac{A_g}{0.2} \right) \left(\frac{\Phi(90^\circ)}{\pi} \right) \left(\frac{S_p}{S_{\oplus}} \right) \left(\frac{R_p}{R_{\oplus}} \right)^2 \left(\frac{R_{\odot}}{R_s} \right)^2 \left(\frac{T_{\text{eff},\odot}}{T_{\text{eff},s}} \right)^4, \quad (2)$$

where T_{eff} is a stellar effective temperature, and values for an Earth-like V-band geometric albedo and phase function (at quadrature) are adopted. Note that it is important to distinguish between planet detection (which is driven by the planet-to-star flux ratio) and atmospheric characterization. The latter requires detecting spectral features (and, possibly, the base of these features), which can be at substantially smaller planet-to-star flux ratios and, owing to the overall faintness of the planet in these features, may drive long integration times. For early, mid, and late M dwarfs, the flux ratio increases dramatically to 2×10^{-9} , 5×10^{-8} , and 4×10^{-7} , respectively. For these cooler stars, though, the small inner working angle that would be needed to resolve the planet from the star drives the need for large-diameter telescopes. Adopting $2\lambda/D$ as a “practical” limit to small inner working angle photometry (Mawet et al 2014), we see that the telescope diameter required to resolve a habitable zone planet from its host is roughly,

$$D > 4 \text{ m} \left(\frac{\lambda}{1 \mu\text{m}} \right) \left(\frac{d}{10 \text{ pc}} \right) \left(\frac{S_p}{S_{\oplus}} \right)^{1/2} \left(\frac{R_{\odot}}{R_s} \right) \left(\frac{T_{\text{eff},\odot}}{T_{\text{eff},s}} \right)^2, \quad (3)$$

where λ is wavelength, D is the telescope diameter, and d is the distance to the system. Returning to the early, mid, and late M dwarf cases, the lower limits on the diameter are 16, 90, and 250 m, respectively.

Secondary Eclipse Spectroscopy: Like transit spectroscopy, secondary eclipse spectroscopy is a differential measurement that requires the combined planetary and stellar flux prior to the planet disappearing behind its host star and comparing this to the stellar flux measured during eclipse (Winn 2010). Here, as was the case for direct imaging, the key quantity is the planet-to-star flux ratio (at full phase). Taking a mid-M dwarf as an example, in reflected light we have,

$$\frac{F_p}{F_s} \approx 0.2 \text{ ppm} \left(\frac{A_g}{0.2} \right) \left(\frac{S_p}{S_{\oplus}} \right) \left(\frac{R_p}{R_{\oplus}} \right)^2 \left(\frac{0.2 \cdot R_{\odot}}{R_s} \right)^2 \left(\frac{2800 \text{ K}}{T_{\text{eff},s}} \right)^4, \quad (4)$$

which is quite small. The characteristic signature size improves at thermal wavelengths, as the planet is self-luminous at these wavelengths. Here, we have the ratio of two blackbodies, and taking the stellar spectrum to be in the Rayleigh-Jeans limit, we have,

$$\frac{F_p}{F_s} \approx 3 \text{ ppm} \left(\frac{R_p}{R_{\oplus}} \right)^2 \left(\frac{0.2 \cdot R_{\odot}}{R_s} \right)^2 \left(\frac{2800 \text{ K}}{T_{\text{eff},s}} \right) \left(\frac{\lambda}{10 \mu\text{m}} \right)^4 \left(\frac{B_{\lambda}(T)}{B_{10 \mu\text{m}}(250 \text{ K})} \right), \quad (5)$$

where B_λ is the Planck function. As was the case for direct imaging, the depths of absorption bands can be as large as the overall signature size (for strong features) or many times smaller (for weak features).

Direct Detection of Surface Liquid Water

Liquids, as opposed to diffusely scattering solid surfaces, have distinct polarization and scattering properties due to the process of Fresnel reflection (Griffiths 1999, p. 382). For a planar surface, the polarization signature peaks at the Brewster angle, where the polarization fraction can approach unity for a liquid with no ripples or waves. This surface will have enhanced reflectivity in the forward scattering direction where the observational angle of reflectance is equal to the solar angle of incidence (i.e., at the specular point), and this reflectivity increases towards glancing angles.

Measurements of the light polarization fraction may be an effective means to detect if an exoplanet has a surface ocean (Williams and Gaidos 2008; Stam 2008). Earthshine and spacecraft observations reveal that Earth’s polarization fraction is a function of the phase angle, peaking at values of 0.2–0.4 in the visible near quadrature (Coffeen 1979). The location of this peak is crescent-ward of the maximum due to Rayleigh scattering, but depends on the wavelength-dependent competition between polarization from Rayleigh, cloud, haze, and ocean scattering (Zugger et al 2010; Vaughan et al 2023). Observing at near-infrared wavelengths will minimize the Rayleigh scattering contributions, pushing the polarization fraction peak to phase angles near those expected for ocean scattering (i.e., near 150°), although peak polarization fractions are likely to still be < 0.2 (Stam 2008; Zugger et al 2011; Vaughan et al 2023).

In addition to polarization, Williams and Gaidos (2008) proposed that specular reflection from an ocean—which is often called “glint”—could be used to detect surface liquid water on exoplanets. Glint would manifest as an increasing planetary reflectivity towards crescent phase, and such an increase has been observed in Earthshine observations (Qiu et al 2003; Pallé et al 2003) and has been used to detect liquid seas in the polar regions of Titan (Stephan et al 2010). Fig. 1 shows apparent albedo spectra of Earth at full and crescent phases, including a crescent phase spectrum where glint is removed.

An increase in reflectivity towards crescent phase is not an unambiguous detection of glint, as forward scattering from clouds, Rayleigh scattering, and geometric effects can all produce a similar behavior. Robinson et al (2010) investigated the extent of the ocean glint effect using a model that included direction-dependent Rayleigh and cloud scattering. This work showed that Rayleigh scattering false positives would be avoided by observing in the near-infrared, where the glinting Earth can be twice as bright as a non-glinting Earth. Since snow/ice reflectivity decreases at longer wavelengths, observing in the near-infrared would also avoid the glint false positive discussed by Cowan et al (2012), which explains a bias towards prob-

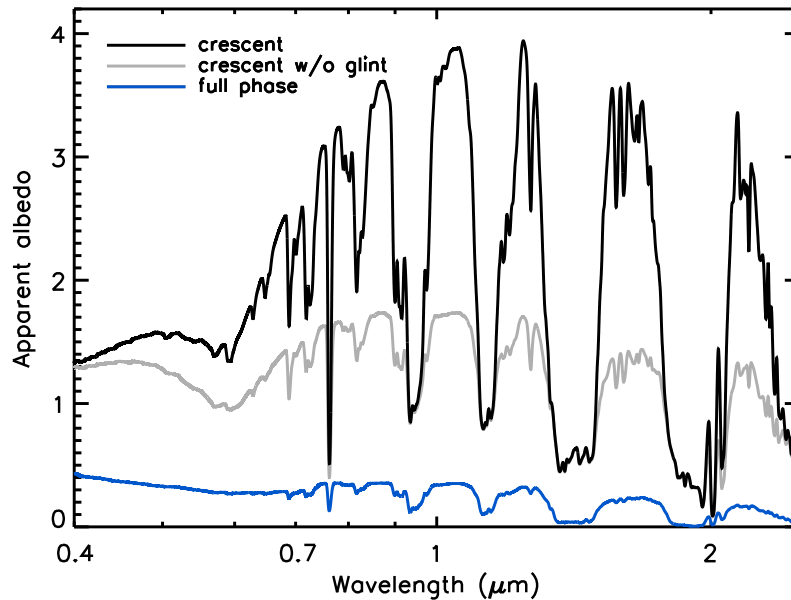


Fig. 1 Apparent albedo of Earth at full phase (blue), and at crescent phase both with glint (black) and without glint (grey), from the validated model described in Robinson et al (2011). Apparent albedo is defined as the albedo a Lambert sphere (with radius equal to the planetary radius) would need to reproduce the observed brightness of the planet, and values larger than unity imply forward scattering.

ing the icy polar regions of a planet at crescent phases. Longitudinal maps made from rotationally-resolved photometry of an Earth-like exoplanet could reveal surface features whose reflectivity increases strongly at crescent phases (Lustig-Yaeger et al 2018), thereby providing another avenue to detect ocean glint effects and rule out surface false positives. The location of the maximum contribution from glint for Earth is near a phase angle of 150° and, for other planets, would depend on cloud cover, atmospheric thickness, and surface wind speeds. As a proof of concept, Robinson et al (2014) were able to detect glint in unresolved *LCROSS* observations of Earth at a phase angle of 130° , although this study benefited from significant *a priori* information.

Spectral information may prove essential for distinguishing between glint and its potential false positives. Robinson (2012) noted that the unique atmospheric path traversed by a glint ray (i.e., two straight-line passes through the atmosphere with a single scattering event at the ocean surface) would imply that a significant portion of the crescent phase spectrum of Earth should resemble a solar spectrum modulated by Rayleigh scattering and gas absorption opacity. Fig. 2 demonstrates this signature. Here, a full phase spectrum of Earth is corrected to crescent phase using a Lambert phase function, and is then subtracted from a crescent phase spectrum of Earth. This difference spectrum, in essence, represents the forward scattering excess (due pri-

marily to clouds and glint) at crescent phase. In wavelength ranges with relatively little gas absorption and, thus, surface sensitivity, the difference spectrum can be well reproduced by a solar spectrum weighted by a term going as $\exp(b/\lambda^4)$ to account for Rayleigh scattering. As a demonstration of this effect, Ryan and Robinson (2022) showed that the characteristic glint-spot spectrum could be detected using spectral principal component analysis on phase-dependent spectral models of Earth, given sufficient orbital access to crescent-phase spectroscopy or photometry.

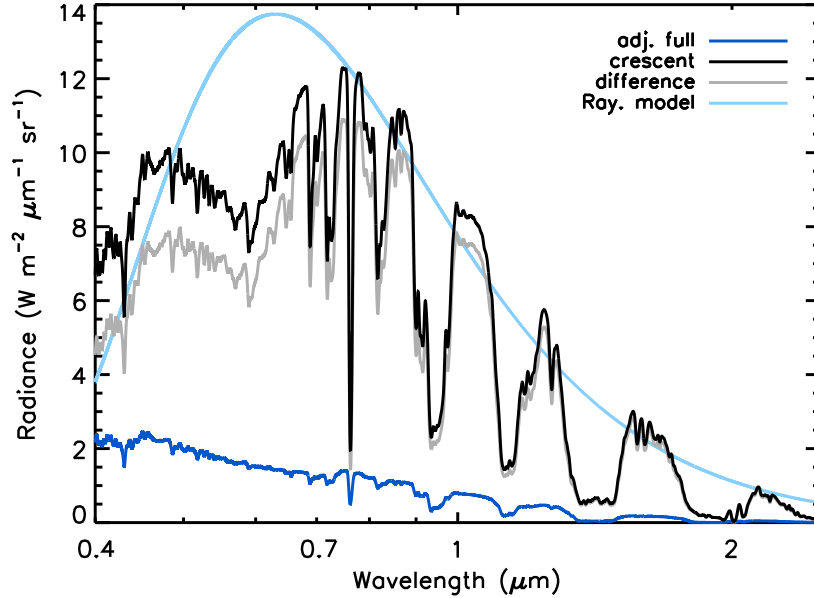


Fig. 2 Spectral signs of glint in phase-dependent observations of Earth. A full phase spectrum of Earth is corrected to crescent phase using a Lambert phase function (dark blue) and subtracted from a crescent phase spectrum of Earth (black) to produce a difference spectrum (grey). The result is well reproduced in window regions by a model that represents a solar spectrum that experiences Rayleigh scattering opacity (light blue) as it passes twice through the atmosphere and scatters once at the surface.

Detecting glint or ocean polarization signatures requires, first and foremost, surface sensitivity and a favorable orbital inclination for the target so that the appropriate phase angles can be accessed. Measuring a polarization fraction of f to a given signal-to-noise ratio (SNR) would require that the individual polarized flux measurements be improved by a factor of $\sqrt{2}/f$, implying the flux measurements be at a SNR of roughly 20 to detect $f \sim 0.2$ at $\text{SNR} = 3$. For the glint reflectivity and polarization signatures, which occur at somewhat extreme crescent phases, detection would require a minimum inclination of about 60° . For such favorable inclinations, resolving an Earth twin at $2\lambda/D$ from a Sun-like host at 10 pc would require an 8 meter diameter telescope (taking $\alpha = 150^\circ$ and $\lambda = 1 \mu\text{m}$). Notably,

both the polarization and glint measurements can be accomplished with broadband observations, which helps to drive down requisite integration times.

Surface Pressure and Temperature

Numerous indicators impart information about pressure and temperature on spectra, although the scale of these signatures can sometimes be quite small. The Rayleigh scattering optical depth is sensitive to the column abundances of primary atmospheric constituents, molecular lines (and bands) are broadened by pressure and thermal effects, and infrared spectra directly indicate the atmospheric and, possibly, surface thermal state. Thus, depending on the wavelength range and observational approach, it is possible to use spectra to make inferences about the pressure and temperature at the surface of an exoplanet, thereby constraining habitability.

For reflected light observations, direct pressure and temperature information will come primarily from the Rayleigh scattering slope and from the widths of molecular bands. Fig. 3 shows reflectivity spectra of worlds with different atmospheric temperatures and pressures where water vapor is the only absorber. The water vapor column mass is Earth-like and held fixed, so that variations are only due to pressure and temperature effects. The influence of atmospheric temperature is rather limited. Pressure, though, has a strong influence on band widths and depths, as well as the scale of the Rayleigh scattering slope. Raman scattering can also indicate atmospheric column density, is most apparent for surface pressures well in excess of 1 bar, and requires measurements at ultraviolet wavelengths (Oklopčić et al 2016)

Our ability to extract pressure information from reflected light spectra will be complicated by uncertainties in planetary mass, planetary radius, the mass(es) of the primary atmospheric constituent(s), and clouds. Nevertheless, inverse models applied to simulated (Feng et al 2018) and real (Robinson and Salvador 2023) reflected light observations of the disk-integrated Earth indicate that spectral data with characteristic SNR of 10 can constrain surface pressure to within an order of magnitude and pushing the data quality to an SNR of 20 constrains the surface pressure to within a factor of 2–3. Complementary studies (Damiano and Hu 2022) with distinct treatments of planetary mass, clouds, and mixing ratio profiles for water vapor demonstrate that the pressure constraint is sensitive to the adopted spectral coverage for the exoplanet analog observation and is also likely sensitive to certain atmospheric parameterizations. Thus the connection between observational SNR and expected constraints on surface pressure remain unclear for Earth-like worlds studied in reflected light. Finally, limited study, outside of nitrogen- or hydrogen-dominated atmospheres, has been given to the dependence of pressure broadened line half widths on the composition of the background atmosphere (e.g., Gamache et al 1997; Hedges and Madhusudhan 2016).

Collision induced absorption features and dimer features—both of which are quite sensitive to background pressure—have been proposed as key indicators of pressure on exoplanets (Misra et al 2014a). Such features have been detected in

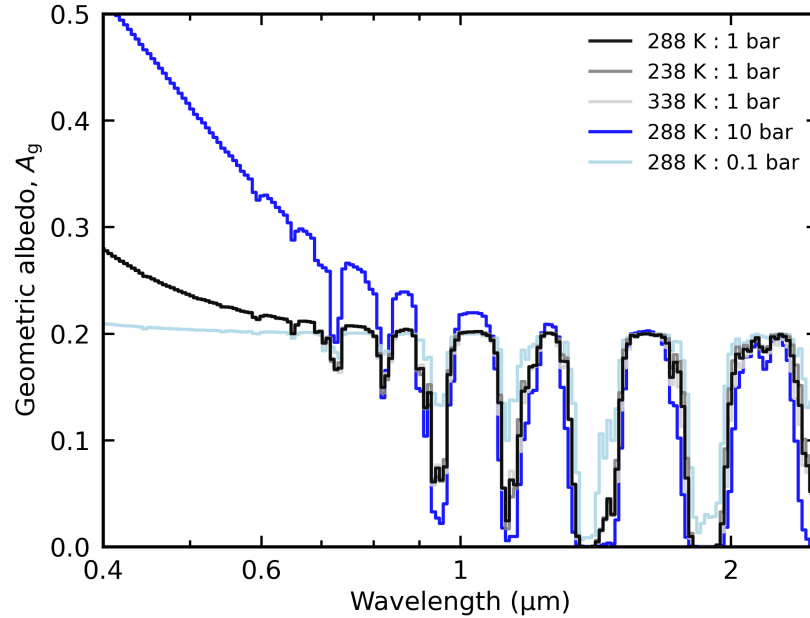


Fig. 3 Reflectivity spectra demonstrating pressure and temperature sensitivities. All cases are clearsky and have the same planetary mass and radius as Earth. Water vapor is the only absorbing gas and its mixing ratio profile is taken to be constant. The column mass of water is fixed as Earth-like across all spectra. The background gas is molecular nitrogen. Temperature effects are shown in grey colors (spanning 100 K) and pressure effects are shown in blue colors (spanning two orders of magnitude).

transmission spectra of Earth’s atmosphere (Pallé et al 2009), and in near-infrared spectra of the Pale Blue Dot (Schwieterman et al 2015). In general, collision induced absorption and dimer features are usually stronger in reflected light and thermal emission spectra, since these techniques tend to probe deeper into atmospheres than transit spectra. Strong molecular nitrogen pressure induced absorption is limited to a feature near $4.3 \mu\text{m}$ (Schwieterman et al 2015), key molecular oxygen features are at 1.06 , 1.27 , and $7 \mu\text{m}$ (Misra et al 2014a), carbon dioxide has a broad feature near $7 \mu\text{m}$ (Baranov et al 2004), and molecular hydrogen has numerous features spanning the visible, near-infrared, and thermal infrared (Frommhold et al 2010; Abel et al 2011).

Transit spectra, through their sensitivity to the atmospheric pressure scale height ($RT/\mu g$, where R is the universal gas constant), contain additional information about temperature (Lecavelier Des Etangs et al 2008), atmospheric mean molecular weight (Benneke and Seager 2012), and, potentially, gravitational acceleration (or mass; de Wit and Seager 2013) (although see Batalha et al 2017). However, while a transit spectrum of an Earth twin would be rich with spectral features (Kaltenegger

and Traub 2009), there are a variety of processes that minimize (or prevent) sensitivity to the surface environment. Fundamental amongst these processes is atmospheric refraction, where rays passing through deeper regions of a planetary atmosphere can experience enough refraction to bend them off the stellar disk (B  tr  mieux and Kaltenegger 2014; Misra et al 2014b). For Earth-like planets around Sun-like stars, refraction prevents sensitivity to the troposphere—although a small amount of the light that passes through the planet’s atmosphere near transit ingress and egress can follow paths that pass near the surface (Misra et al 2014b).

Transit spectra of Earth twins around mid- or late-M dwarfs are much less affected by refraction, so, here, clouds and gas opacity are the primary impediment to surface sensitivity. Large slant pathlengths associated with the transit geometry cause spectral regions with only a small amount of vertical optical depth to become opaque. This issue is especially true for clouds and hazes (Fortney 2005), which tend to have optical depths that vary slowly in wavelength, and can thus block observations of the deep atmosphere over wide spectral ranges (e.g., Kreidberg et al 2014; Knutson et al 2014; Robinson et al 2014). Aerosol extinction in transit spectra would be significant for a hazy early Earth (Arney et al 2016), and even modern Earth, which is generally thought to have “patchy” clouds, is >70% cloud-covered when thin, high-altitude cirrus clouds are considered (Stubenrauch et al 2013). Fig. 4 shows transit spectra of Earths around different host star types, and includes the effects of realistic clouds and refraction.

Achieving the types of transit observations outlined in this section is made difficult by detector noise and systematics and clouds. Greene et al (2016) showed that a single visit with *James Webb Space Telescope (JWST)*, with an assumed set of instrument systematic noise floors, is unlikely to be able to place strong constraints on the atmospheric properties of a warm (500 K) super-Earth planet with a steam atmospheres transiting an M0 dwarf. By pushing to a mid-M dwarf host, Benneke and Seager (2012) concluded that *JWST* could place constraints on the surface pressure of a similarly warm super-Earth planet with an atmosphere dominated by molecular nitrogen. The Benneke and Seager (2012) results did not address clouds, refraction, detector systematics, or cooler (Earth-like) atmospheres, all of which will make detections of surface pressure more difficult. Most promisingly, de Wit and Seager (2013) found that *JWST* could constrain pressures and temperatures for a cloud-free Earth-like planet orbiting a late-M dwarf using 200 hr of in-transit observation time, although potential degeneracies may exist (Batalha et al 2017). Early transit observations of Earth-sized worlds orbiting late M-type stars with *JWST* have not yet yielded atmospheric constraints and indicate that substantial investments of observing time will be required to obtain effective reconnaissance of these atmospheres (Lim et al 2023).

A limited number of studies exist that address the information content (especially with regard to surface pressure and temperature) of directly observed emission spectra from Earthlike exoplanets. Using retrieval techniques to fit simulated observations of a cloud-free Earth in the thermal infrared, von Paris et al (2013) showed that surface temperatures and pressures for Earth-like planets could be constrained to within the habitable range with spectral resolving power ($\mathcal{R} = \lambda/\Delta\lambda$) greater

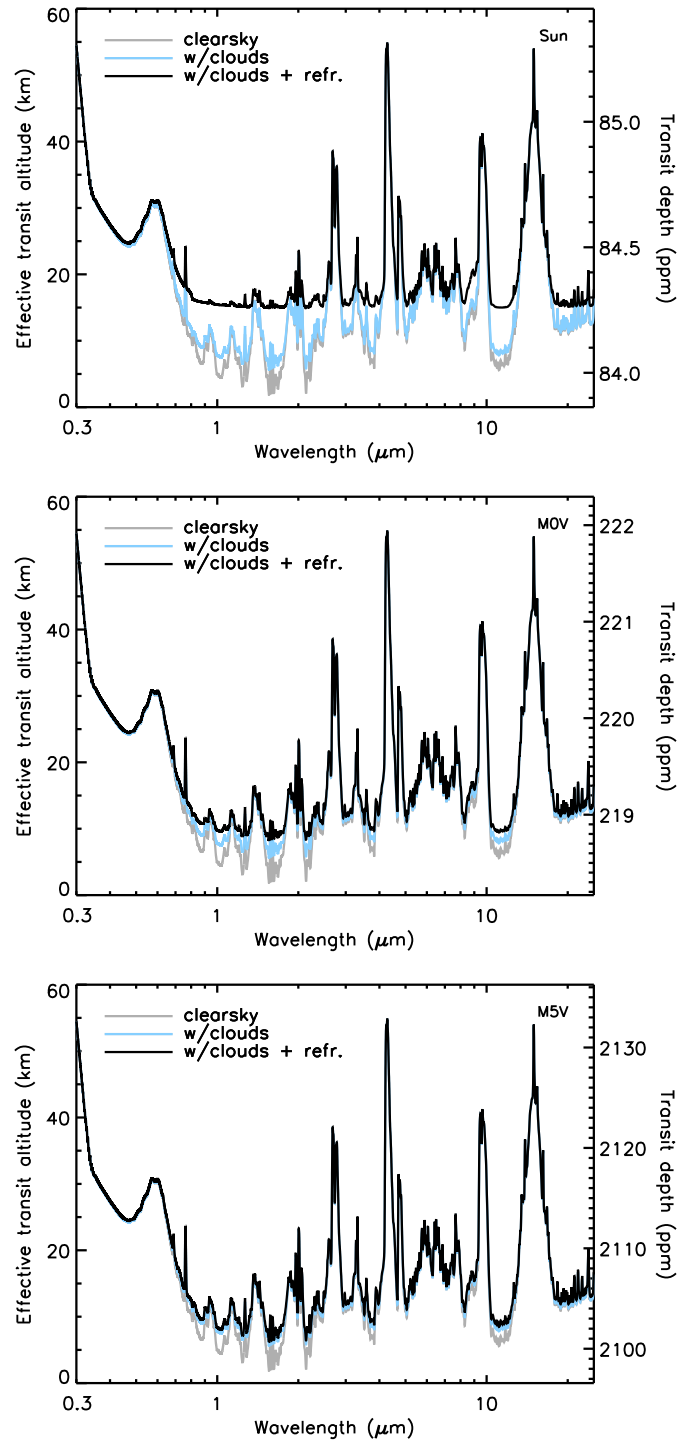


Fig. 4 Transit spectra of an Earth twin around a Sun-like, M0 dwarf, and M5 dwarf host. Clearsky cases are in grey, blue curves show the addition of realistic clouds, and black curves contain both clouds and refraction. From a transit spectra model described in Robinson (2017).

than roughly 10 and SNRs greater than roughly 10, although these estimates are likely optimistic given the cloud-free assumption made in this work. More-recent cloud-free inverse modeling studies in support of the Large Interferometer For Exoplanets (LIFE) mission concept—a space-based mid-infrared interferometer capable of imaging and characterizing rocky worlds in the habitable zone of nearby stars (Quanz et al 2022)—indicate that larger SNRs (greater than roughly 20) might be required to constrain surface temperatures to be above the water freezing point (Alej et al 2022). Retrieval studies applied in the thermal infrared to Earth-like worlds that do include clouds tend to agree with the requirement of SNRs larger than roughly 20 for strong surface temperature constraints (Robinson and Salvador 2023).

Other Habitability Indicators

A variety of observations, while not direct confirmations of habitability, could also be used as evidence for liquid water at/near the surface of an exoplanet. Within this area, the topic that has seen the most study is that of photometric variability. At visible wavelengths, contrast between Earth's reflective clouds and its surface—which is absorptive due to the large ocean coverage fraction—makes our planet the most variable in the Solar System (Ford et al 2001), with peak-to-trough diurnal variations typically of order 20% (Livengood et al 2011).

Rotationally resolved, visible wavelength observations of the Pale Blue Dot could be used to produce surface feature maps (Cowan et al 2009; Fujii et al 2011; Cowan et al 2011), and lightcurves resolved over longer timescales could indicate variability due to weather. (Lightcurves at thermal wavelengths could also reveal variability due to weather, but have received little study.) Similar observations for a distant Earth-like planet, coupled with information about the planetary orbit (or insolation), would likely argue for atmospheric water vapor condensation, although the condensate phase (liquid or solid) and whether or not the aerosols reach a surface in a liquid state would be difficult to discern. Confirmation, or detection, of the presence of liquid droplets, as well as their composition, could come from reflectance and polarization measurements at phase angles corresponding to maximum scattering from the primary rainbow of the droplets (Bailey 2007; Vaughan et al 2023), although accessing these phase angles requires orbital inclinations like those needed for glint measurements.

Detecting other signs of water vapor condensation, especially near an exoplanetary surface, would make for stronger indications of habitability. Fujii et al (2013) used rotationally resolved spectra of the Pale Blue Dot to detect differences in the spatial distribution of water vapor and molecular oxygen in Earth's atmosphere. Since molecular oxygen is well-mixed, this detection argues for a non-uniform vertical and horizontal distribution of water vapor, where the most likely interpretation for a potentially habitable exoplanet would be exchange between the gas and liquid/solid phase. More recently, Robinson and Marley (2016) noted that retrieval of a water vapor mixing ratio profile that is larger near an exoplanetary surface, or the re-

trieval of a condensate cloud layer located near the surface of a potentially habitable exoplanet, would argue for stable surface liquid or solid water. Recent inverse modeling applied to synthetic reflected light observations of Earthlike worlds reveals that detecting signs of structure in a water vapor profile will be extremely challenging, possibly requiring SNRs larger than 20 for both optical and near-infrared coverage (Damiano and Hu 2022).

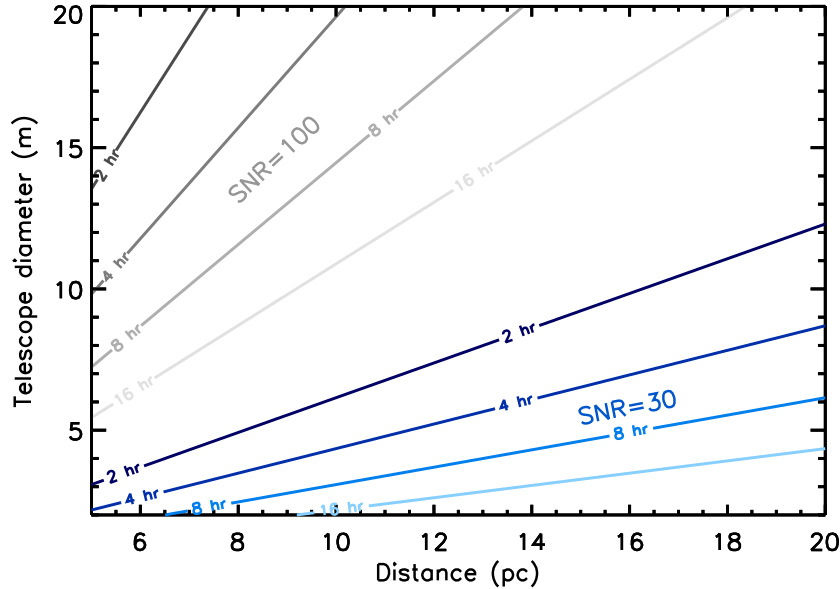


Fig. 5 Contours of integration time required to achieve a SNR of 100 (grey) and 30 (blue) for Earth twins in V band as a function of telescope diameter and distance to the planetary system. Only noise from stellar leakage (at a raw contrast of 10^{-10}), Solar System zodiacal light, and exozodiacal light (at the level of three exozodis) are considered. Models assume a Sun-like host, and relevant expressions are given in Robinson et al (2016). Achieving a SNR of 100 would be strongly limited by systematic noise floors.

Mapping of Pale Blue Dots is made difficult by the requisite SNRs, and, potentially, the need for simultaneous photometry in multiple bands (although these bands can be wide, which helps to increase the signal from the planet). Cowan and Strait (2013) use diurnal lightcurves at a SNR of 100 to map the Pale Blue Dot without prior information for surface or cloud spectra, although simply detecting changing cloud patterns may only require SNRs larger than roughly 20–30. Fig. 5 shows how the integration time required for V band photometry depends on distance to the system and telescope diameter. If SNRs of 100 are required within 2–4 hr (for rotational resolution), then mapping will be limited to only very nearby targets. However, if mapping can be accomplished with lower SNRs, then targets out to much larger distances can be accessed, even with modest-sized telescopes. Finally, note that re-

trieving water vapor or cloud profiles from reflected light observations will also require high-SNR observations, at least if the jovian cloud retrievals mentioned in the previous section are indicative.

Outstanding Challenges

Table 1 Key Habitability Observables and Constraints for Earth Twins.

Observable	Technique	Wavelength	Noise Req.	Add'l Considerations
glint	direct imaging	0.7–2.5 μm	SNR $\gtrsim 3$	broadband; $i \gtrsim 60^\circ$
polarization	direct imaging	0.7–2.5 μm	SNR $\gtrsim 20$	broadband; $i \gtrsim 10^\circ$
	transit	0.4–30 μm	$\lesssim 10\text{--}50$ ppm	$\mathcal{R} \gtrsim 100$; mid/late-M dwarf
surface p & T	direct imaging	0.4–2.5 μm	SNR $\gtrsim 20$ (?)	$\mathcal{R} \gtrsim 100$; no T constraint
	direct imaging	4–30 μm	SNR $\gtrsim 20$	$\mathcal{R} \gtrsim 10$
weather/mapping	direct imaging	0.4–1 μm	SNR $\gtrsim 30\text{--}100$	broadband
H ₂ O/cloud profiles	direct imaging	0.4–2.5 μm	SNR $\gtrsim 20$ (?)	$\mathcal{R} \gtrsim 100$

While a variety of techniques and observables relevant to characterizing habitability have been proposed, key questions still remain about the feasibility and utility of these different methods. Regarding the direct detection of surface liquid water, requisite integration times for realistic observing scenarios have seldom been explored (although see Lustig-Yaeger et al 2018; Ryan and Robinson 2022). Performing these observations in the near-infrared (where stars are fainter) may prove costly, and noise from observing near the inner working angle (for glint) or from polarized light from exozodiacal dust will both introduce complications. Similarly, SNRs (which dictate integration times) required for retrieving water vapor and cloud profiles from reflection, emission, and/or transmission spectra of realistic Pale Blue Dots also remain largely unexplored. Finally, future work on variability should focus on the wavelength range, timing, and minimum required SNRs to do mapping. Table 1 presents an overview of the current understanding of the observing requirements for the different approaches to detecting or constraining habitability.

Once observational feasibility has been addressed, a more holistic discussion of characterizing for habitability should emerge. This will be especially true for high contrast imaging. Here, repeat observations may be required to confirm the planetary nature of a target and to constrain the orbit (and, thus, insolation) of a confirmed planet. It is unclear if certain observational tests for habitability should be worked into the confirmation and orbit determination sequence. Also, following this sequence, open questions remain regarding the order in which different observations

(e.g., glint, polarization, moderate resolution spectroscopy) should take place. Such questions can only be settled by weighing the information supplied by these different observations with the time required to achieve them.

Conclusions

Detecting or constraining the habitability of a distant exoplanet will be a challenging and critical step towards understanding the frequency of the origin of life on other worlds. Transit spectroscopy, secondary eclipse observations, and high contrast imaging all have the potential to reveal key planetary properties related to habitability, and these techniques each have their own assets and challenges. Reflected light observations can directly reveal surface liquid water, either through polarization or glint measurements. Constraints on surface pressure are possible with most observational techniques (depending on wavelength coverage), but surface temperatures (which, when combined with a surface pressure measurement, can demonstrate habitability) will prove difficult to measure in reflected light. Detecting water vapor condensation at/near a surface is also feasible, either through spectral retrieval of gas mixing ratio or condensate profiles, or through mapping using time resolved photometric measurements. In the end, though, it could prove that no unambiguous “smoking gun” exists for detecting stable surface liquid water, so that actual constraints on habitability may come from multiple lines of evidence using a variety of approaches brought to bear on a distant Pale Blue Dot.

Acknowledgements TR gratefully acknowledges support from NASA through the Sagan Fellowship Program executed by the NASA Exoplanet Science Institute. The results reported herein benefitted from collaborations and/or information exchange within NASA’s Nexus for Exoplanet System Science (NExSS) research coordination network sponsored by NASA’s Science Mission Directorate. Certain essential tools used in this work were developed by the NASA Astrobiology Institute’s Virtual Planetary Laboratory, supported by NASA under Cooperative Agreement No. NNA13AA93A. TR thanks J Fortney for a constructive critique of this review.

References

- Abe Y Matsui T (1988) Evolution of an Impact-Generated H₂O-CO₂ Atmosphere and Formation of a Hot Proto-Ocean on Earth. *Journal of Atmospheric Sciences* 45:3081–3101
- Abe Y, Abe-Ouchi A, Sleep NH Zahnle KJ (2011) Habitable Zone Limits for Dry Planets. *Astrobiology* 11:443–460
- Abel M, Frommhold L, Li X Hunt KLC (2011) Collision-Induced Absorption by H₂ Pairs: From Hundreds to Thousands of Kelvin. *Journal of Physical Chemistry A* 115:6805–6812
- Alei, E, Konrad, BS, Angerhausen, D, et al (2022) Large Interferometer For Exoplanets (LIFE). V. Diagnostic Potential of a Mid-Infrared Space Interferometer for Studying Earth Analogs. *A&A* 665:A106
- Arney G, Domagal-Goldman SD, Meadows VS et al (2016) The Pale Orange Dot: The Spectrum and Habitability of Hazy Archean Earth. *Astrobiology* 16:873–899

- Bailey J (2007) Rainbows, Polarization, and the Search for Habitable Planets. *Astrobiology* 7:320–332
- Baranov YI, Lafferty WJ, Fraser GT (2004) Infrared Spectrum of the Continuum and Dimer Absorption in the Vicinity of the O₂ Vibrational Fundamental in O₂/CO₂ Mixtures. *Journal of Molecular Spectroscopy* 228:432–440
- Batalha NE, Kempton EM, Mbarek R (2017) Challenges to Constraining Exoplanet Masses via Transmission Spectroscopy. *ApJ* 836:L5
- Beichman CA, Woolf NJ, Lindensmith CA (eds) (1999) *The Terrestrial Planet Finder: A NASA Origins Program to Search for Habitable Planets*. NASA Jet Propulsion Laboratory
- Benneke B, Seager S (2012) Atmospheric retrieval for super-Earths: Uniquely constraining the atmospheric composition with transmission spectroscopy. *The Astrophysical Journal* 753(2):100
- Bétrémieux Y, Kaltenegger L (2014) Impact of Atmospheric Refraction: How Deeply Can We Probe Exo-Earth's Atmospheres During Primary Eclipse Observations? *ApJ* 791:7
- Borucki WJ, Koch D, Basri G et al (2010) Kepler Planet-Detection Mission: Introduction and First Results. *Science* 327:977
- Brack A (1993) Liquid Water and the Origin of Life. *Origins of Life and Evolution of the Biosphere* 23:3–10
- Brown TM (2001) Transmission spectra as diagnostics of extrasolar giant planet atmospheres. *The Astrophysical Journal* 553(2):1006
- Cash W, Schindhelm E, Arenberg J et al (2007) External Occulters for Direct Observation of Exoplanets: An Overview. In: *UV/Optical/IR Space Telescopes: Innovative Technologies and Concepts III*, Proc SPIE, vol 6687, p 668712
- Chyba CF, Phillips CB (2001) Special Feature: Possible ecosystems and the search for life on Europa. *Proceedings of the National Academy of Science* 98:801–804
- Coffeen DL (1979) Polarization and Scattering Characteristics in the Atmospheres of Earth, Venus, and Jupiter. *Journal of the Optical Society of America* (1917-1983) 69:1051–1064
- Cowan NB, Traut TE (2013) Determining Reflectance Spectra of Surfaces and Clouds on Exoplanets. *ApJ* 765:L17
- Cowan NB, Agol E, Meadows VS et al (2009) Alien Maps of an Ocean-bearing World. *ApJ* 700:915–923
- Cowan NB, Robinson T, Livengood TA et al (2011) Rotational Variability of Earth's Polar Regions: Implications for Detecting Snowball Planets. *ApJ* 731:76–+
- Cowan NB, Abbot DS, Voigt A (2012) A False Positive for Ocean Glint on Exoplanets: The Latitude-Albedo Effect. *ApJ* 752:L3
- Cowan NB, Greene T, Angerhausen D et al (2015) Characterizing Transiting Planet Atmospheres through 2025. *PASP* 127:311–327
- Damiano, M, Hu, R (2022) Reflected Spectroscopy of Small Exoplanets II: Characterization of Terrestrial Exoplanets. *AJ* 163:299
- Dole SH (1964) *Habitable Planets for Man*. Blaisdell, New York
- Drossart P, Rosenqvist J, Encrenaz T et al (1993) Earth Global Mosaic Observations with NIMS-Galileo. *Planet Space Sci* 41:551–561
- Feng, YK, Robinson, TD, Fortney, JJ, et al (2018) Characterizing Earth Analogs in Reflected Light: Atmospheric Retrieval Studies for Future Space Telescopes. *AJ* 155:200
- Ford EB, Seager S, Turner EL (2001) Characterization of Extrasolar Terrestrial Planets from Diurnal Photometric Variability. *Nature* 412:885–887
- Forget F, Pierrehumbert RT (1997) Warming Early Mars with Carbon Dioxide Clouds That Scatter Infrared Radiation. *Science* 278:1273
- Fortney JJ (2005) The effect of condensates on the characterization of transiting planet atmospheres with transmission spectroscopy. *Monthly Notices of the Royal Astronomical Society* 364(2):649–653
- Fronnhold L, Abel M, Wang F et al (2010) Infrared Atmospheric Emission and Absorption by Simple Molecular Complexes, From First Principles. *Molecular Physics* 108:2265–2272
- Fujii Y, Kawahara H, Suto Y et al (2011) Colors of a Second Earth. II. Effects of Clouds on Photometric Characterization of Earth-like Exoplanets. *ApJ* 738:184

- Fujii Y, Turner EL Suto Y (2013) Variability of Water and Oxygen Absorption Bands in the Disk-integrated Spectra of Earth. *ApJ* 765:76
- Galilei G (1632) Dialogue Concerning the Two Chief Worlds Systems. Giovanni Battista Landini
- Gamache RR, Lynch R, Plateaux JJ Barbe A (1997) Halfwidths and Line Shifts of Water Vapor Broadened by CO₂: Measurements and Complex Robert-Bonamy Formalism Calculations. *J Quant Spectr Rad Transf* 57:485–496
- Goldblatt C, Robinson TD, Zahnle KJ Crisp D (2013) Low Simulated Radiation Limit for Runaway Greenhouse Climates. *Nature Geoscience* 6:661–667
- Greene TP, Line MR, Montero C et al (2016) Characterizing transiting exoplanet atmospheres with jwst. *The Astrophysical Journal* 817(1):17
- Griffiths DJ (1999) Introduction to Electrodynamics (3rd Ed.). Prentice Hall
- Guyon O, Pluzhnik EA, Kuchner MJ, Collins B Ridgway ST (2006) Theoretical Limits on Extrasolar Terrestrial Planet Detection with Coronagraphs. *ApJS* 167:81–99
- Haqq-Misra JD, Domagal-Goldman SD, Kasting PJ Kasting JF (2008) A Revised, Hazy Methane Greenhouse for the Archean Earth. *Astrobiology* 8:1127–1137
- Hart MH (1978) The Evolution of the Atmosphere of the Earth. *Icarus* 33:23–39
- Hart MH (1979) Habitable Zones about Main Sequence Stars. *Icarus* 37:351–357
- Hedges C Madhusudhan N (2016) Effect of Pressure Broadening on Molecular Absorption Cross Sections in Exoplanetary Atmospheres. *MNRAS* 458:1427–1449
- Huang SS (1959) Occurrence of life in the universe. *American Scientist* 47(3):397–402
- Hubbard W, Fortney J, Lunine J et al (2001) Theory of extrasolar giant planet transits. *The Astrophysical Journal* 560(1):413
- Joshi MM, Haberle RM Reynolds RT (1997) Simulations of the Atmospheres of Synchronously Rotating Terrestrial Planets Orbiting M Dwarfs: Conditions for Atmospheric Collapse and the Implications for Habitability. *Icarus* 129:450–465
- Kaltenegger L Traub W (2009) Transits of earth-like planets. *The Astrophysical Journal* 698:519
- Kaltenegger L, Selsis F, Fridlund M et al (2010) Deciphering Spectral Fingerprints of Habitable Exoplanets. *Astrobiology* 10:89–102
- Kasting JF, Whitmire DP Reynolds RT (1993) Habitable Zones around Main Sequence Stars. *Icarus* 101:108–128
- Knutson HA, Benneke B, Deming D Homeier D (2014) A Featureless Transmission Spectrum for the Neptune-Mass Exoplanet GJ 436b. *Nature* 505:66–68
- Kopparapu RK, Ramirez R, Kasting JF et al (2013) Habitable Zones around Main-sequence Stars: New Estimates. *ApJ* 765:131
- Kopparapu, RK, Wolf, ET, Meadows, VS (2020) Characterizing Exoplanet Habitability. In: Meadows VS et al (eds) *Planetary Astrobiology*, University of Arizona Press, Tucson, pp 449–476
- Kreidberg L, Bean JL, Désert JM et al (2014) Clouds in the atmosphere of the super-earth exoplanet gj 1214b. *Nature* 505(7481):69–72
- Lecavelier Des Etangs A, Pont F, Vidal-Madjar A Sing D (2008) Rayleigh scattering in the transit spectrum of hd 189733b. *Astronomy and Astrophysics* 481:L83–L86
- Leconte J, Forget F, Charnay B et al (2013) 3D Climate Modeling of Close-In Land Planets: Circulation Patterns, Climate Moist Bi-Stability, and Habitability. *A&A* 554:A69
- Lim, O, Benneke, B, Doyon, R, et al (2023) Atmospheric Reconnaissance of TRAPPIST-1 b with JWST/NIRISS: Evidence for Strong Stellar Contamination in the Transmission Spectra. *ApJ* 955:L22.
- Livengood TA, Deming LD, A’Hearn MF et al (2011) Properties of an Earth-Like Planet Orbiting a Sun-Like Star: Earth Observed by the EPOXI Mission. *Astrobiology* 11:907–930
- Luger R Barnes R (2015) Extreme Water Loss and Abiotic O₂ Buildup on Planets Throughout the Habitable Zones of M Dwarfs. *Astrobiology* 15:119–143
- Lustig-Yaeger, J, Meadows, VS, Tovar Mendoza, G, et al (2018) Detecting Ocean Glint on Exoplanets Using Multiphase Mapping. *AJ* , 156:301
- Matsui T Abe Y (1986) Impact-Induced Atmospheres and Oceans on Earth and Venus. *Nature* 322:526–528

- Mawet D, Pueyo L, Lawson P et al (2012) Review of Small-Angle Coronagraphic Techniques in the Wake of Ground-Based Second-Generation Adaptive Optics Systems. In: *Space Telescopes and Instrumentation 2012: Optical, Infrared, and Millimeter Wave*, Proc SPIE , vol 8442, p 844204
- Mawet D, Milli J, Wahhaj Z et al (2014) Fundamental Limitations of High Contrast Imaging Set by Small Sample Statistics. *ApJ* 792:97
- Meadows VS (2010) Planetary Environmental Signatures for Habitability and Life. In: Mason J (ed) *Exoplanets: Detection, Formation, Properties, Habitability*, Springer, Berlin, pp 259–284
- Misra A, Meadows V, Claire M Crisp D (2014a) Using Dimers to Measure Biosignatures and Atmospheric Pressure for Terrestrial Exoplanets. *Astrobiology* 14:67–86
- Misra A, Meadows V Crisp D (2014b) The Effects of Refraction on Transit Transmission Spectroscopy: Application to Earth-like Exoplanets. *ApJ* 792:61
- Oklopčić, A, Hirata, CM, Heng, K (2016) Raman Scattering by Molecular Hydrogen and Nitrogen in Exoplanetary Atmospheres *ApJ* 832:30
- Pallé E, Goode PR, Yurchyshyn V et al (2003) Earthshine and the Earth's Albedo: 2. Observations and Simulations over Three Years. *Journal of Geophysical Research (Atmospheres)* 108:4710
- Pallé E, Osorio MRZ, Barrena R, Montañés-Rodríguez P Martín EL (2009) Earth's transmission spectrum from lunar eclipse observations. *Nature* 459(7248):814–816
- Pappalardo RT, Belton MJS, Breneman HH et al (1999) Does Europa have a Subsurface Ocean? Evaluation of the Geological Evidence. *J Geophys Res* 104:24,015–24,056
- Pierrehumbert R Gaidos E (2011) Hydrogen Greenhouse Planets Beyond the Habitable Zone. *ApJ* 734:L13
- Qiu J, Goode P, Pallé E et al (2003) Earthshine and the earth's albedo: 1. earthshine observations and measurements of the lunar phase function for accurate measurements of the earth's bond albedo. *J Geophys Res* 108(4709):1999–2007
- Quanz, SP, Ottiger, M, Fontanet, E et al (2022) Large Interferometer For Exoplanets (LIFE). I. Improved Exoplanet Detection Yield Estimates for a Large Mid-Infrared Space-Interferometer Mission. *A&A* 664:A21.
- Ramirez RM Kaltenecker L (2014) The Habitable Zones of Pre-main-sequence Stars. *ApJ* 797:L25
- Rasool SI de Bergh C (1970) The Runaway Greenhouse and the Accumulation of CO₂ in the Venus Atmosphere. *Nature* 226:1037–1039
- Robinson TD (2012) Simulating and characterizing the pale blue dot. PhD thesis, University of Washington
- Robinson TD (2017) A Theory of Exoplanet Transits with Light Scattering. *ApJ* p submitted
- Robinson TD Marley MS (2016) Constraining Planetary Habitability: A LUVVOIR Science Draft Case. Tech. rep., NASA Goddard Space Flight Center
- Robinson, TD, Salvador, A (2023) Exploring and Validating Exoplanet Atmospheric Retrievals with Solar System Analog Observations. *Planet Sci J* 4:10
- Robinson TD, Meadows VS Crisp D (2010) Detecting Oceans on Extrasolar Planets Using the Glint Effect. *ApJ* 721:L67–L71
- Robinson TD, Meadows VS, Crisp D et al (2011) Earth as an Extrasolar Planet: Earth Model Validation Using EPOXI Earth Observations. *Astrobiology* 11:393–408
- Robinson TD, Ennico K, Meadows VS et al (2014) Detection of Ocean Glint and Ozone Absorption Using LCROSS Earth Observations. *ApJ* 787:171
- Robinson TD, Maltagliati L, Marley MS Fortney JJ (2014) Titan solar occultation observations reveal transit spectra of a hazy world. *Proceedings of the National Academy of Sciences* 111(25):9042–9047
- Robinson TD, Stapelfeldt KR Marley MS (2016) Characterizing Rocky and Gaseous Exoplanets with 2 m Class Space-based Coronagraphs. *PASP* 128(2):025,003
- Rugheimer S, Kaltenecker L, Zsom A, Segura A Sasselov D (2013) Spectral Fingerprints of Earth-like Planets Around FGK Stars. *Astrobiology* 13:251–269
- Ryan, DJ, Robinson, TD (2022) Detecting Oceans on Exoplanets with Phase-dependent Spectral Principal Component Analysis. *Planet Sci J* 3:33

- Sagan C, Thompson WR, Carlson R, Gurnett D, Hord C (1993) A Search for Life on Earth from the Galileo Spacecraft. *Nature* 365:715–721
- Schwieterman EW, Robinson TD, Meadows VS, Misra A, Domagal-Goldman S (2015) Detecting and Constraining N₂ Abundances in Planetary Atmospheres Using Collisional Pairs. *ApJ* 810:57
- Seager S, Sasselov D (2000) Theoretical transmission spectra during extrasolar giant planet transits. *The Astrophysical Journal* 537(2):916
- Selsis F, Kasting JF, Levrard B et al (2007) Habitable Planets around the Star Gliese 581? *A&A* 476:1373–1387
- Shaklan SB, Noecker MC, Glassman T et al (2010) Error Budgeting and Tolerancing of Starshades for Exoplanet Detection. In: *Space Telescopes and Instrumentation 2010: Optical, Infrared, and Millimeter Wave*, Proc SPIE, vol 7731, p 77312G
- Shields AL, Meadows VS, Bitz CM et al (2013) The Effect of Host Star Spectral Energy Distribution and Ice-Albedo Feedback on the Climate of Extrasolar Planets. *Astrobiology* 13:715–739
- Stam DM (2008) Spectropolarimetric Signatures of Earth-like Extrasolar Planets. *A&A* 482:989–1007
- Stephan K, Jaumann R, Brown RH et al (2010) Specular Reflection on Titan: Liquids in Kraken Mare. *Geophys Res Lett* 37:L07104
- Stevenson DJ (1999) Life-Sustaining Planets in Interstellar Space? *Nature* 400:32
- Stubenrauch CJ, Rossow WB, Kinne S et al (2013) Assessment of Global Cloud Datasets from Satellites: Project and Database Initiated by the GEWEX Radiation Panel. *Bulletin of the American Meteorological Society* 94:1031–1049
- Traub WA, Oppenheimer BR (2010) Direct Imaging of Exoplanets. In: Seager S (ed) *Exoplanets*, University of Arizona Press, Tucson, pp 111–156
- Vaughan, SR, Gebhard, TD, Bott, K et al (2023) Chasing Rainbows and Ocean Glints: Inner Working Angle Constraints for the Habitable Worlds Observatory. *MNRAS* 524:5477
- von Paris P, Gebauer S, Godolt M et al (2010) The Extrasolar Planet Gliese 581d: A Potentially Habitable Planet? *A&A* 522:A23
- von Paris P, Hedelt P, Selsis F, Schreier F, Trautmann T (2013) Characterization of potentially habitable planets: Retrieval of atmospheric and planetary properties from emission spectra. *A&A* 551:A120
- Way MJ, Del Genio AD, Kiang NY et al (2016) Was Venus the first habitable world of our solar system? *Geophys Res Lett* 43(16):8376–8383
- Whitmire DP, Reynolds RT, Kasting JF (1991) Habitable Zones for Earth-like Planets Around Main Sequence Stars. In: Heidmann J, Klein MJ (eds) *Bioastronomy: The Search for Extraterrestrial Life—The Exploration Broadens*, Lecture Notes in Physics, Berlin Springer Verlag, vol 390, pp 173–178
- Williams DM, Gaidos E (2008) Detecting the Glint of Starlight on the Oceans of Distant Planets. *Icarus* 195:927–937
- Winn JN (2010) Exoplanet Transits and Occultations. In: Seager S (ed) *Exoplanets*, University of Arizona Press, Tucson, pp 55–77
- de Wit J, Seager S (2013) Constraining exoplanet mass from transmission spectroscopy. *Science* 342(6165):1473–1477
- Wolf ET, Toon OB (2013) Hospitable Archean Climates Simulated by a General Circulation Model. *Astrobiology* 13:656–673
- Wordsworth R, Pierrehumbert R (2013) Hydrogen-Nitrogen Greenhouse Warming in Earth's Early Atmosphere. *Science* 339:64
- Yang J, Cowan NB, Abbot DS (2013) Stabilizing Cloud Feedback Dramatically Expands the Habitable Zone of Tidally Locked Planets. *ApJ* 771:L45
- Zsom A, Seager S, de Wit J, Stamenković V (2013) Toward the Minimum Inner Edge Distance of the Habitable Zone. *ApJ* 778:109
- Zugger ME, Kasting JF, Williams DM, Kane TJ, Philbrick CR (2010) Light Scattering from Exoplanet Oceans and Atmospheres. *ApJ* 723:1168

Zugger ME, Kasting JF, Williams DM, Kane TJ Philbrick CR (2011) Searching for Water Earths in the Near-Infrared. *ApJ* 739:12